J. Biomechanics Vol. 24, No. 12, pp. 1095–1105, 1991.
Printed in Great Britain

0021-9290/91 $3.00 + .00
Pergamon Press plc

CALCULATION OF VERTICAL GROUND REACTION FORCE ESTIMATES DURING RUNNING FROM POSITIONAL DATA

MAARTEN F. BOBBERT, HENK C. SCHAMHARDT and BENNO M. NIGG
Human Performance Laboratory, Faculty of Physical Education, University of Calgary, Canada

Abstract—The purpose of this study was to calculate, as a function of time, segmental contributions to the vertical ground reaction force F_z from positional data for the landing phase in running. In order to evaluate the accuracy of the method, time histories of the sum of the segmental contributions were compared to $F_z(t)$ measured directly by a force plate.

The human body was modeled as a system of seven rigid segments. During running the positions of markers defining these segments were monitored using a video analysis system operating at 200 Hz. Special care was taken to minimize marker movement relative to the mass centers of segments, and low-pass cutoff frequencies of 50 Hz (markers defining leg segments) and 15–20 Hz (markers defining upper body) were used in filtering the position time histories so as to ensure that high signal frequencies were preserved. The magnitude of the high-frequency peak in F_z, also known as 'impact force peak', was estimated with errors $< 10\%$, while the time of occurrence of the peak was estimated with errors < 5 ms. It would appear that the positional data were sufficiently accurate to be used for calculation of intersegmental forces and moments during the landing phase in running.

Analysis of the segmental contributions to $F_z(t)$ revealed that the first peak in F_z has its origin in the contribution of support leg segments, while its magnitude is determined primarily by the contribution of the rest of the body. These contributions could be varied independently by changing running style. It follows that if the possible relationship between 'impact force peaks' and injuries is to be investigated, or if the effects of running shoe and surface construction on these force peaks are to be evaluated, the calculation of segmental contributions to $F_z(t)$ is a more suitable approach than measuring only $F_z(t)$.

INTRODUCTION

A large portion of today's population is aware of the benefits to be gained from being physically fit, and numerous individuals rely on running as a means to acquire and retain their fitness. Because of the increase in the number of runners and the mileage covered, clinicians nowadays are frequently facing patients with running injuries. Unfortunately, as the etiology of many injuries is unknown, the development of prevention and treatment modalities is severely hampered.

It seems reasonable to assume that at least some running injuries are associated with the landing phase where the body, so to speak, collides with the ground. In this phase the muscles which control the movement are forcibly lengthened, which could cause them to develop large forces and high internal stresses. Large muscular forces may also cause high stresses in the tendons which transmit these forces and in their bony attachments. The landing phase is also the phase where runners who strike the ground first with their rearfoot produce the so-called 'impact force peaks': high-frequency force peaks in the time histories of the vertical ground reaction force F_z occurring in the first 50 ms of ground contact (Cavanagh and Lafortune, 1980; Frederick *et al.*, 1981; Dickinson *et al.*, 1985; Nigg *et al.*, 1987). If the joints of animals are regularly submitted to such high-frequency force peaks, degenerative changes take place in articular cartilage and subchondral bone (Dekel and Weissman, 1978; Radin *et al.*, 1973, 1978; Serink *et al.*, 1977). Based on these findings, several authors have speculated that impact transients on heel strike in walking may lead to degeneration of articular cartilage, osteoarthritis and low back pain (Light *et al.*, 1980; Wosk and Voloshin, 1981; Voloshin and Wosk, 1982). Analogously, it has been speculated that 'impact force peaks' play a role in the development of pain and injuries in runners (e.g. James *et al.*, 1978; Clement *et al.*, 1981).

If we assume that phenomena occurring during the landing phase in running are involved in the etiology of injuries, a mechanical analysis of this phase, including estimates of intersegmental forces and moments, becomes desirable. In order to make such an analysis, estimates are required of inertial and gravitational force contributions. This necessitates the assessment of mass distribution in the body segments under consideration, as well as estimation of translational and rotational displacements and accelerations. In biomechanical studies, the latter accelerations are usually obtained by double differentiation of positional data in the time domain, and it would be very convenient if the same procedure could be followed for the landing phase in running. However, the high-frequency peaks in $F_z(t)$ reflect high-frequency peaks in

Received in final form 30 *May* 1991.
Address for correspondence: Maarten F. Bobbert, Vrije Universiteit, Vakgroep Functionele Anatomie, Faculteit der Bewegingswetenschappen, v.d. Boechorststraat 9, 1081 BT Amsterdam, The Netherlands.

the time histories of accelerations of body segments, and the reconstruction of such peaks is only possible if a high signal-to-noise ratio exists in the positional data. Thus, the question arises whether it is possible to obtain positional data of sufficient accuracy for a mechanical analysis of the landing phase.

The present study is a first step towards providing a mechanical description of the landing phase in running. The purpose of the study is to calculate as a function of time the segmental contributions to F_z using accelerations estimated from positional data. In order to evaluate the accuracy of the method, time histories of the sum of the segmental contributions, henceforth referred to as calculated $F_z(t)$, were compared to $F_z(t)$ measured directly by a force plate. A few of the results of this study were published earlier (Bobbert and Schamhardt, 1989).

METHODS

Outline of setup and procedures

Using Newton's second law of motion for a single, rigid body, it may be derived that:

$$F_z = m_B(\ddot{z}_{MCB} - g), \quad (1)$$

where F_z is the vertical component of the ground reaction force vector (forces directed upward are defined as positive), m_B is the body mass, g is the acceleration due to gravity ($-9.81\ ms^{-2}$), and $\ddot{z}_{MCB}$ is the vertical component of the acceleration of the body's mass center (upward accelerations are defined as positive). If the body is subdivided into n rigid segments, equation (1) may be written as:

$$F_z = \sum_{i=1}^{n} m_i(\ddot{z}_i - g), \quad (2)$$

where m_i is the mass of the ith segment and $\ddot{z}_i$ is the vertical acceleration of the ith segment. In this study, seven body segments were defined; the two feet, the two lower legs, the two upper legs, and a segment comprising head, arms and trunk (HAT). The segment locations were derived from the three-dimensional positions of retroflective spheres, monitored using four video cameras and a high-speed video-analysis system. Landmark position time histories were smoothed and differentiated twice to obtain accelerations. The latter were used in combination with literature data on magnitudes and locations of segmental masses (Clauser *et al.*, 1969) to calculate F_z according to equation (2). The calculated $F_z(t)$ curves were compared to $F_z(t)$ curves measured using a force plate.

The comparison between calculated and measured $F_z(t)$ curves was made for three male subjects (masses of 65, 69 and 77 kg), each of whom performed several running trials wearing personal shoes. Running speed and running style were varied across trials so as to obtain a broad spectrum of ground reaction force time histories.

Details on methods and procedures are provided below.

Collection of force data

Ground reaction forces were recorded using a KISTLER type 9287 force plate (Kistler Instrumente AG, Winterthur, Switzerland), which was installed according to the manufacturer's specifications. The force plate was connected to an electronic amplifier unit (KISTLER type 9861A, Kistler Instrumente AG, Winterthur, Switzerland), and the eight output signals of this unit were sampled at 1000 Hz using a data acquisition board (DT2821-F-16SE, Data Translation Inc., Marlborough, MA) and a personal computer (COMPAQ Portable III, Compaq Computer Corp., Houston, TX). The analog F_z output of the amplifier was fed to a circuit including a light emitting diode (LED) in view of one of the video cameras. The threshold in the circuit was such that the LED came on when F_z exceeded 20 N.

Collection of video data

Video data were collected using a VP310 videorecorder (Motion Analysis Corporation, Santa Rosa, CA) and four electronically shuttered cameras (NAC MOS V-14 Camera 60/220 F/S) equipped with 12–120 mm zoom lenses (Angénieux, Paris, France). Camera positions are shown schematically in Fig. 1. A 1000 W lamp was placed directly behind each camera. The cameras were zoomed in as far a possible to a volume of 2 m in x (fore–aft axis), 1 m in y (mediolateral axis) and 2 m in z (vertical axis), with the center of the base area corresponding to the center of the force plate. This volume was subsequently calibrated using 16 control points and Expert Vision three-dimensional software.

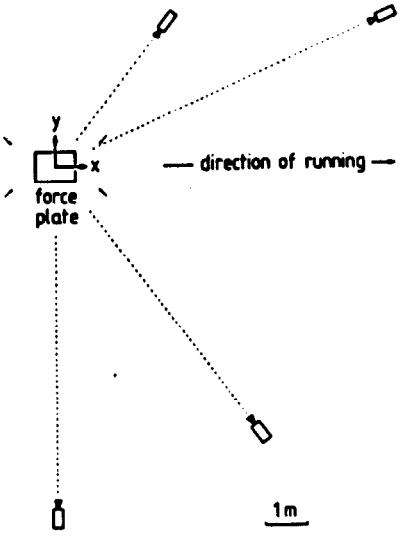

Fig. 1. Positions of cameras used for collecting positional data. Arrows indicate the corners of the base of the calibrated volume.

During running, data were collected at 200 Hz, the maximum sampling frequency of the system. For synchronization of video data with force data, the LED described above was used. The first video frame on which the LED appeared was supposed to correspond in time to the second force sample following the sample where F_z had exceeded the 20 N threshold. Since force data were collected at 1000 Hz, synchronization errors ranged from -3 to $+2$ ms.

Positions of retroflective markers

Movement of the skin relative to the underlying tissue is one of the major sources of error if high-frequency force peaks are to be reconstructed from positional data. Extensive pilot work was devoted to minimizing this source of error. The problem manifested itself especially in the leg segments. If retroflective markers (spheres with a diameter of 2 cm) were applied directly to the skin overlying the ankle, knee and hip joints, the distance between adjacent markers varied during running, even if long straps of athletic tape were used to fix the markers to a large area of skin. Figure 2 shows for the stance phase in running an example of time histories of distances between skin markers in the support leg. Both low-frequency and high-frequency fluctuations with an amplitude of >2 cm can be observed in the tracings. The high-frequency fluctuations immediately after touch-down were of primary concern because they were expected to cause major errors in accelerations of leg segments calculated by double differentiation of the marker position time histories.

In order to solve the problem of skin movement relative to the underlying tissue, a device was constructed consisting of two light wooden rods connected by a hinge joint. The hinge joint was aligned with the estimated flexion–extension axis of the knee joint (at the height of the lateral collateral ligament, 2 cm above the tibial plateau), one rod was fastened to the lower leg and one to the upper leg using athletic tape and elastic bandages. Markers were subsequently fixed to the wooden rods at the height of the estimated plantarflexion–dorsiflexion axis of the ankle joint (on the lateral malleolus, 0.5 cm anterior to its tip), the axis of the hinge joint, and the estimated axis of anteversion–retroversion of the hip joint (2 cm proximal of the greater trochanter). Thus, the distance between markers defining the lower leg and the distance between markers defining the upper leg was forced to be constant. Obviously, the setup simplified motion of the upper leg with respect to the lower leg to rotation about an axis passing through the marker on the hinge joint. This has the *disadvantage* that the possible effects of compression of structures in the knee joint on the acceleration of the upper leg with respect to the lower leg cannot be studied. A great *advantage* of connecting the rods was, however, that a much better fixation of the rod on the upper leg could be achieved.

The device consisting of the two rods and the hinge joint was used in both lower extremities. In addition, two markers were applied to the shoe of the support leg, one at the height of the 5th metatarsophalangeal joint, the other at the height of the tuber calcanei. In the upper body, one marker was taped to the skin at the height of the sternum (with long strips of athletic tape running from below the sternum diagonally across the thorax, over the neck, to the shoulder blades) and one marker was fixed on top of the head (using an elastic band passing under the chin). The latter two markers were retroflective spheres with a diameter of 4 cm. The marker positions are shown schematically in Fig. 3.

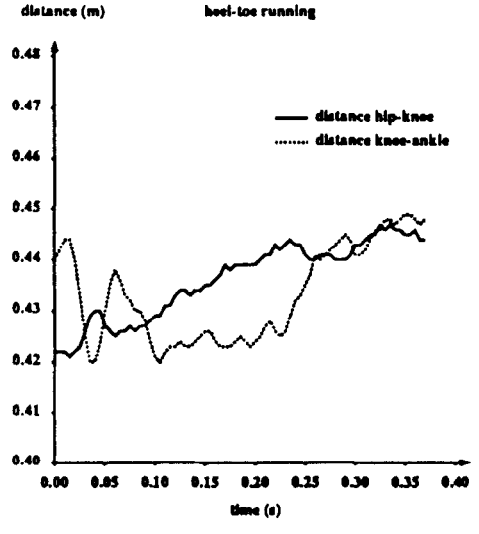

Fig. 2. Time histories of distances between skin markers at the height of the ankle, knee and hip joints of the support leg. Long strips of athletic tape were used to fix the markers to a large area of skin.

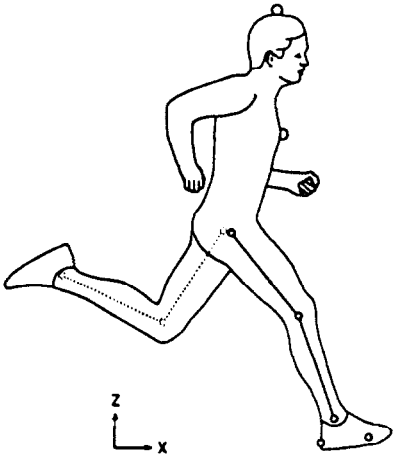

Fig. 3. Locations of markers used to define the positions of body segments.

Processing of video data

Time histories of marker positions were determined using Expert Vision three-dimensional software. The vertical coordinates were smoothed by running them twice (once forward, once backward) through a Butterworth 2nd order filter and differentiating twice using a direct 3-point (first central difference) derivative routine. Because the digitizing process was automated and fast, boundary effects could be minimized by extending the marker histories with 15 frames preceding touch-down and 15 frames following toe-off.

The vertical force contributions of the segments, $m_i(\Xi_i - g)$, were determined from the marker accelerations using data reported by Clauser *et al.* (1969) on segmental masses (expressed in terms of percentages of body masses) and positions of segmental mass centers (expressed in terms of percentages of segment lengths). For the vertical acceleration of the foot of the swinging leg the vertical acceleration of the ankle marker on that leg was used. In order to obtain the vertical acceleration of HAT, the average of the vertical accelerations of the two hip markers, the marker on the sternum and the marker on the head was used. Movements of the arms relative to the trunk were not restricted. It had been found in pilot work that their influence on the calculated $F_z(t)$ was negligible.

Frequency content of $F_z(t)$ *in running*

A requirement for successful calculation of ground reaction forces from positional data is, of course, that the sampling frequency of 200 Hz is high enough to handle the frequency content of the force peaks which occur in the landing phase. In pilot work an attempt was made to answer the question whether this requirement was met. A Fourier analysis of ground reaction force time histories gave no conclusive evidence. A more or less continuous spectrum was found, in which amplitudes of >2% of the maximum amplitude were present up to 52 Hz and amplitudes of >1% occurred up to 70 Hz. Therefore, a different approach was selected. The measured $F_z(t)$ was integrated twice to obtain a relatively noise-free 1000 Hz 'position' time history [re. equation (1)]. The sampling frequency of this time history was reduced from 1000 to 200 Hz by selecting every fifth point, and the result was filtered and differentiated twice to recalculate the force time history. Figure 4 shows an example of the results. It is obvious that with a sampling frequency of only 200 Hz some attenuation of force peaks occurs. This is caused by the effect of a reduction of sampling frequency on the low-pass nature of the estimator for the second time derivative (see Woltring, 1984). The attenuation of the double differentiator used in the present study was:

$$H_2(\omega T) = \left(\frac{\sin(2\pi f T)}{2\pi f T}\right)^2, \qquad (3)$$

where f is signal frequency and T is the time between

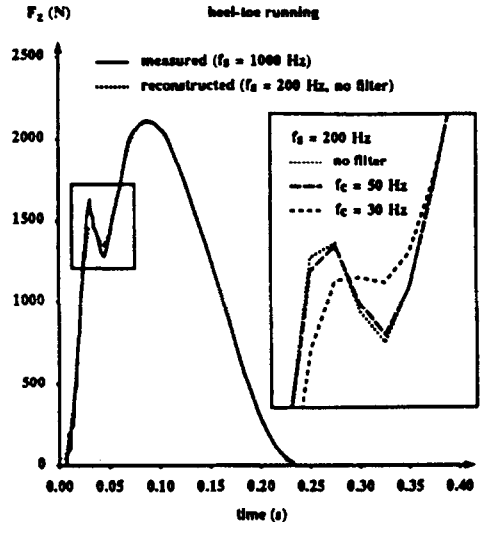

Fig. 4. Influence of sampling frequency f_s and low-pass cutoff frequency f_c on reconstructed time histories of the vertical ground reaction force $F_z(t)$. To obtain the reconstructed curve the measured $F_z(t)$ signal, sampled at 1000 Hz, was integrated twice to derive a 1000 Hz 'position' time history. The sample frequency of this time history was reduced to 200 Hz by selecting every fifth point, and the outcome was filtered and differentiated twice.

adjacent samples [for the derivation of equation (3), see Appendix]. For a 200 Hz sampling frequency ($T = 0.005$) the attenuation at 50 Hz signal frequency is 0.405. In spite of this the sharp force peak after landing is preserved (Fig. 4), indicating that, given the choice of the derivative estimator, a sampling frequency of 200 Hz is high enough. It should be noted here that at the same sampling frequency, acceleration peaks may be reconstructed even better using analytical differentiation with a natural, complete or periodic spline, as discussed by Woltring (1985).

The next step was to examine the influence of the cutoff frequency. Lowering the cutoff frequency from 200 to 50 Hz has a negligible effect on the reconstructed force time history, as might have been expected from what is said above. The force peak disappears, however, if the cutoff frequency is dropped to 30 Hz. From this finding it was concluded that, in order for the calculation of ground reaction forces from positional data to be successful, high frequencies should be preserved in marker position histories.

Accuracy in collecting and processing positional data

In the previous paragraph the effects of sampling frequency and cutoff frequency were determined using a relatively noiseless position time history, obtained by double differentiation of the $F_z(t)$ curve which was to be reconstructed. Needless to say, cutoff frequencies as high as 50 Hz can only be used if the signal-to-noise ratio is acceptable up to this frequency. In order to test this for positional data collected in this study, a 4 cm wide strip of retroflective tape was wrapped around

the center of a hollow metal rod (length = 1.8 m; dia = 2 cm; mass = 2.5 kg), and the rod was dropped vertically on a rubber mat covering the force plate. The setup used in collecting and processing force and video data was the same as that used in the actual running experiments. Figure 5 shows a typical example of measured and calculated $F_z(t)$ curves. The experiment stimulates a 'worst case' of the impact force peaks found in running experiments; the total duration of the measured contact phase is only 25 ms. In spite of the fact that only four or five video frames contained information about the impact, the correspondence between the calculated and measured $F_z(t)$ curves was acceptable. It is interesting to note here that a more 'fair' comparison is made if the calculated $F_z(t)$ curve is compared to the measured curve after processing the latter as described in the previous paragraph (integrating the measured 1000 Hz $F_z(t)$ curve twice, reducing the sampling frequency to 200 Hz by taking every fifth point, filtering at the 50 Hz cutoff frequency used for the kinematic data, and differentiating twice). In that case the calculated and measured curves become virtually identical (results are not shown), indicating that the spatio-temporal resolution of the high-speed video-analysis system is appreciable (see also Furnée, 1989).

From the results presented above, it seems warranted to conclude that the proposed method of calculating $F_z(t)$ from marker position time histories is sufficiently accurate for reconstruction of high-frequency force peaks that occur during the landing phase in running. Of course, *the application of the method can be successful only if the changes in marker positions reflect changes in positions of segmental mass centers.*

RESULTS

Comparison of calculated and measured $F_z(t)$ *curves*

Figure 6 shows an example of the segment positions, projected on the sagittal plane, as a function of time. The runner moves from left to right. The fact that the attitude of the upper body remains virtually constant during the whole cycle supports the decision to compute the acceleration of HAT by simply averaging the accelerations of the hip markers, the marker on the sternum and the marker on the head.

Figure 7 shows the effect of lowering the cutoff frequency of the Butterworth filter f_c on the outcome of the comparison of calculated and measured $F_z(t)$. If all marker position time histories are filtered with $f_c = 50$ Hz, extremely large fluctuations occur in the calculated $F_z(t)$. When f_c is set to 10 Hz for all markers position histories the fluctuations disappear, but so does the first force peak, as was expected (Fig. 4). A good correspondence between measured and calculated $F_z(t)$ during the first 50 ms could be obtained with the following combination of cutoff frequencies: 50 Hz for foot, ankle and knee markers, 20 Hz for hip markers, and 15 Hz for markers on the sternum and head. The rationale for using an intermediate f_c for smoothing hip marker position time histories was that these are utilized both in the calculation of the accelerations of relatively light segments (the upper legs) and in the calculation of the acceleration of the heavy mass (HAT). By trying out several other combinations of cutoff frequencies, it was confirmed that the selection of a high f_c for markers defining leg segments and a low one for other markers was the crucial step; the outcome was relatively insensitive to the specific values of the cutoff frequencies.

Running speed and style were varied across running trials in such a way that a wide variety of ground reaction force time histories was obtained. A good

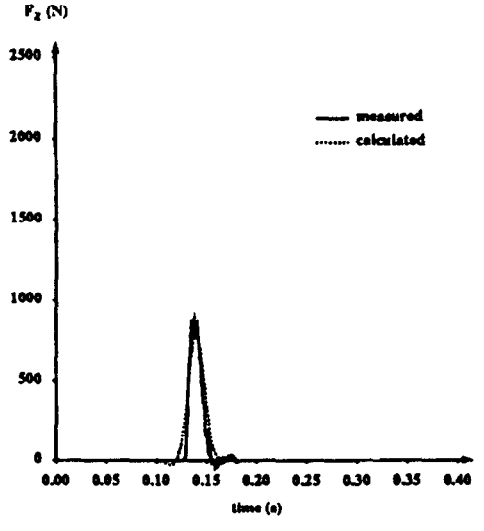

Fig. 5. Examples of measured and calculated time histories of the vertical ground reaction force $F_z(t)$ for a hollow metal rod bouncing on a rubber mat.

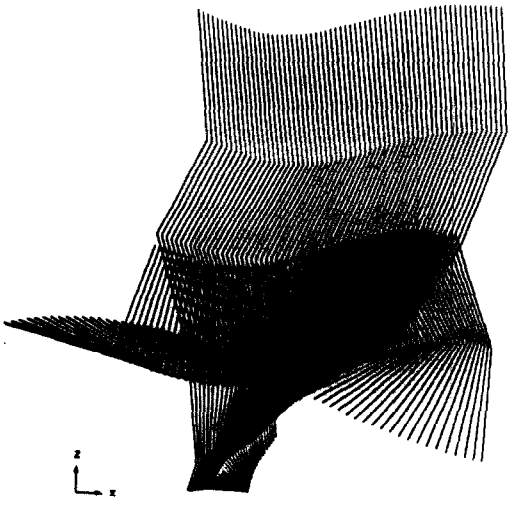

Fig. 6. Example of marker positions, projected on the sagittal plane (xz plane), as a function of time. The subject is running from left to right.

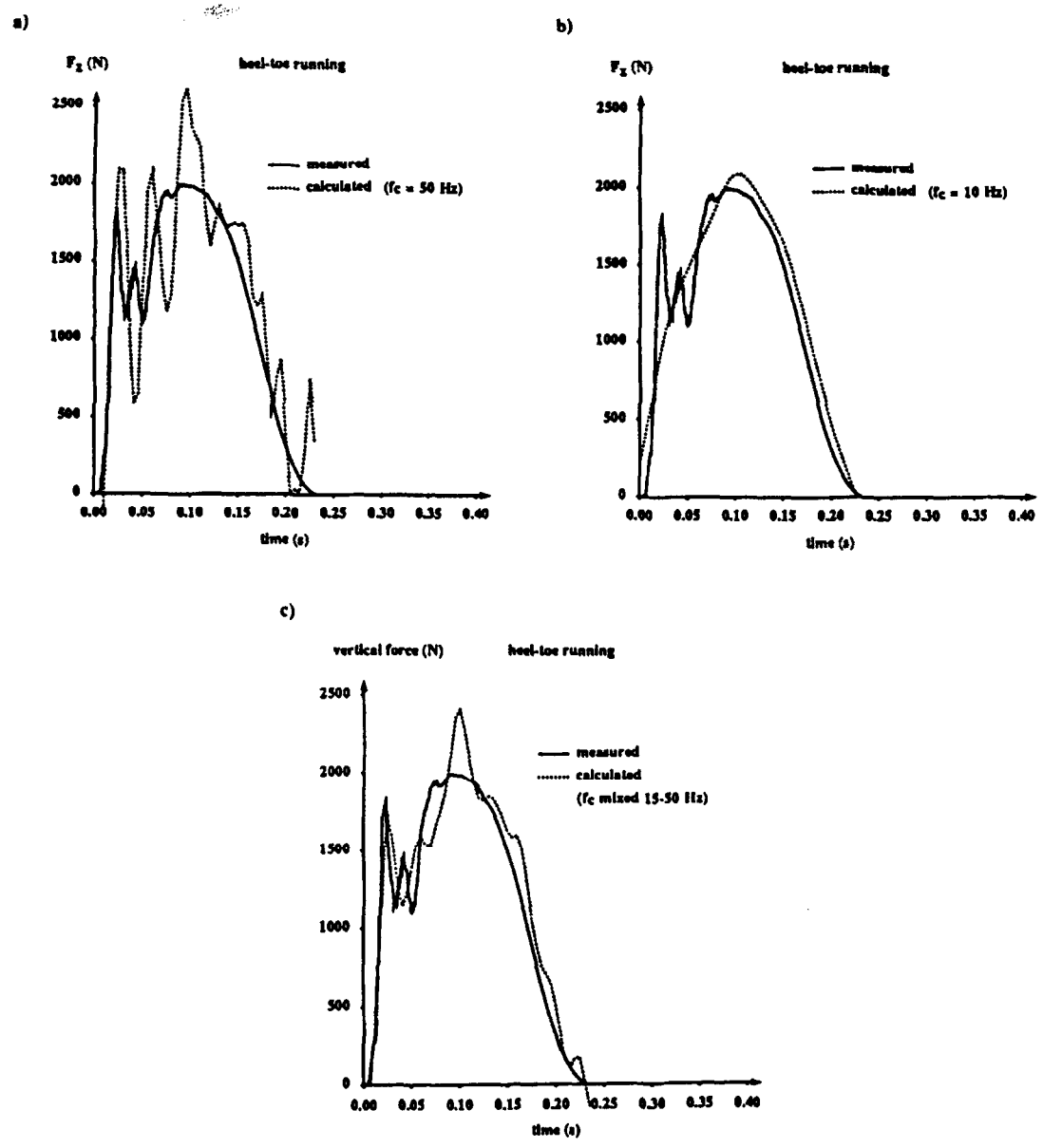

Fig. 7. Effects of lowering the low-pass cutoff frequency f_c on time histories of the vertical ground reaction force $F_z(t)$ calculated from positional data. In (a) all marker positions histories were filtered using $f_c = 50$ Hz, in (b) they were filtered using $f_c = 10$ Hz. In (c) f_c was 15 Hz for the markers on the sternum and head, 20 Hz for the hip markers, and 50 Hz for all other markers.

correspondence between measured and calculated $F_z(t)$ during the first 50 ms was achieved in all trials. Examples are shown in Fig. 8(a–f). In general, the magnitude of the first peak in $F_z(t)$ was calculated from the positional data with errors $< 10\%$, but in some trials the time of occurrence of the peak was delayed up to 5 ms in the calculated $F_z(t)$ relative to the measured $F_z(t)$ [e.g. Fig. 8(f)]. By relating the time of occurrence to the instant of ground contact, it was confirmed that the delay was not due to errors in the synchronization of film and force plate data. The variations in $F_z(t)$ immediately following the first peak could *not* always be calculated accurately from the position time histories [e.g. Fig. 8(e)]. Such variations in $F_z(t)$ did not occur in toe-running where the force peak immediately after landing was absent [Fig. 8(d)].

A sensitivity analysis revealed that it made little difference whether the swing leg was incorporated separately or was simply considered to have the same acceleration as the HAT. Given this finding, a setup with more than one camera is no longer strictly needed. Using only the results from the lateral camera (see Fig. 1), reasonably accurate force calculations could be obtained as well. This is shown in Fig. 9(a, b), which compares the calculated $F_z(t)$ time histories in Fig. 8(a, b) with histories obtained using results of the lateral camera only. It should be mentioned that in many trials the marker on the sternum was lost from

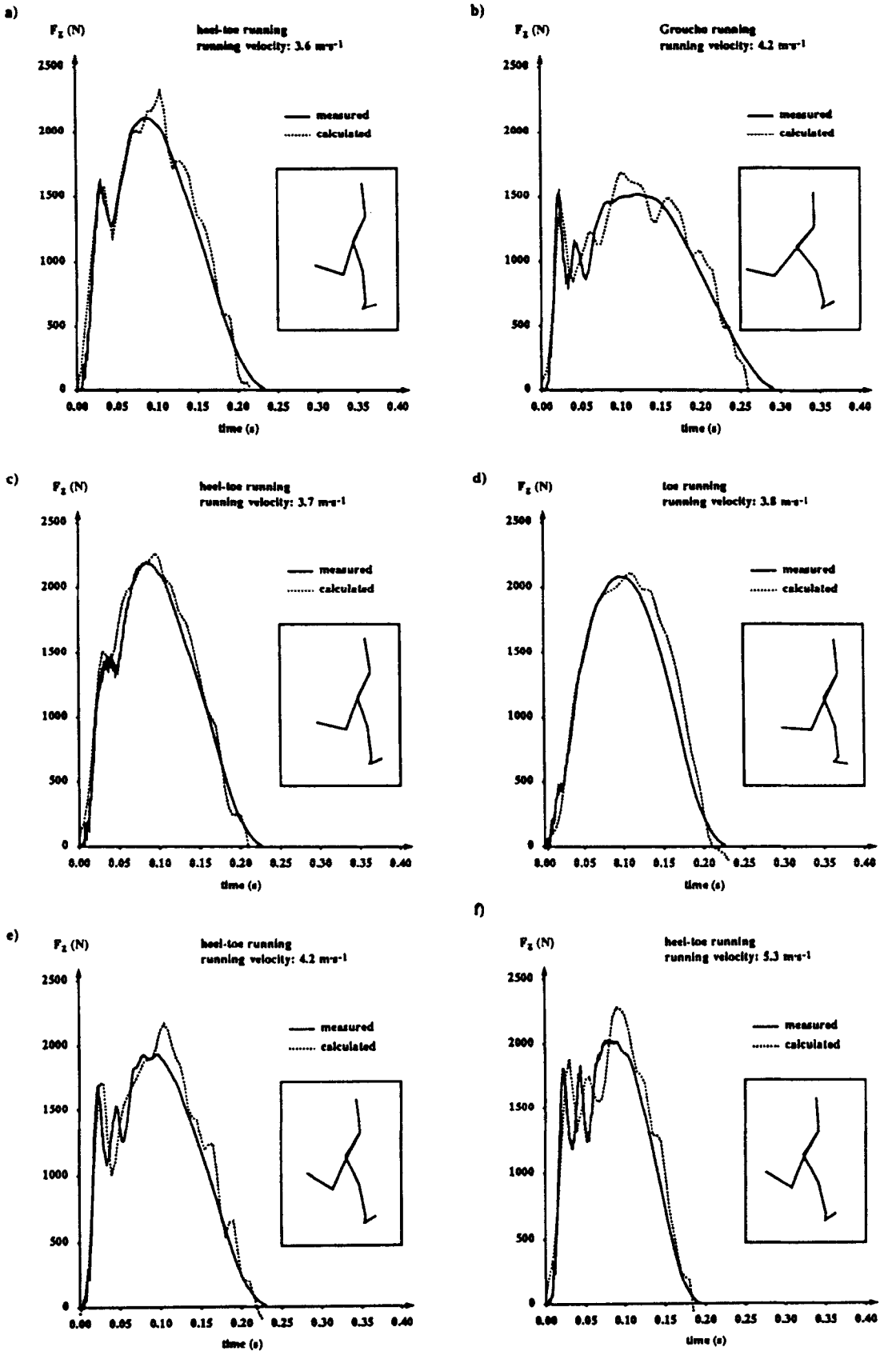

Fig. 8. Examples of measured and calculated time histories of the vertical ground reaction force $F_z(t)$. The cutoff frequencies used in calculating $F_z(t)$ from positional data were the same as in Fig. 7(c). The inset of each graph shows the orientation of body segments in the sagittal plane at touch-down.

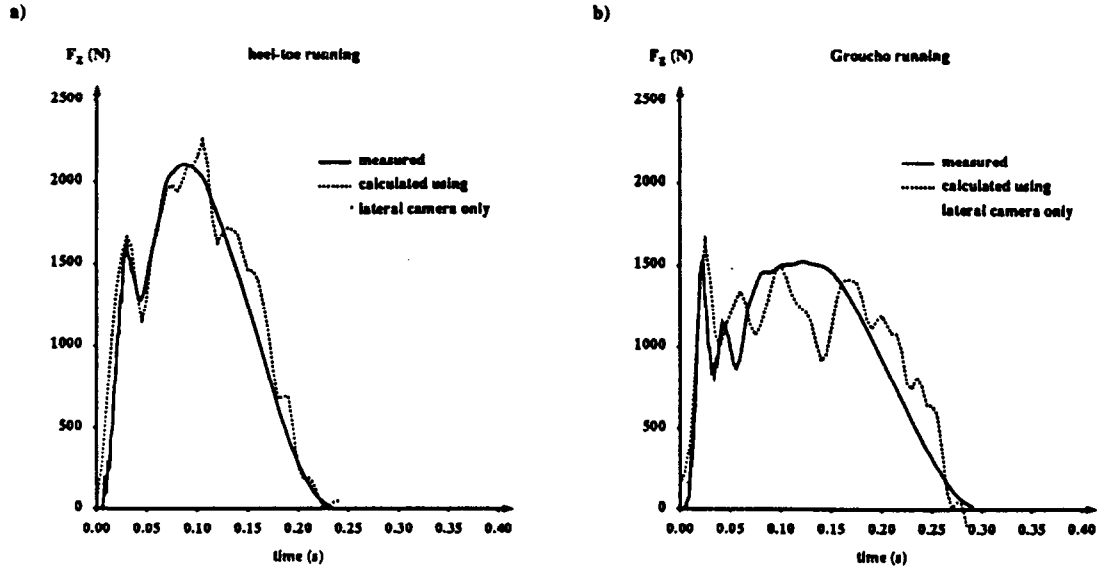

Fig. 9. Examples of measured and calculated time histories of the vertical ground reaction force $F_z(t)$. Calculated curves were obtained using positional data of the lateral camera. Results in (a) and (b) correspond to results in (a) and (b) of Fig. 8.

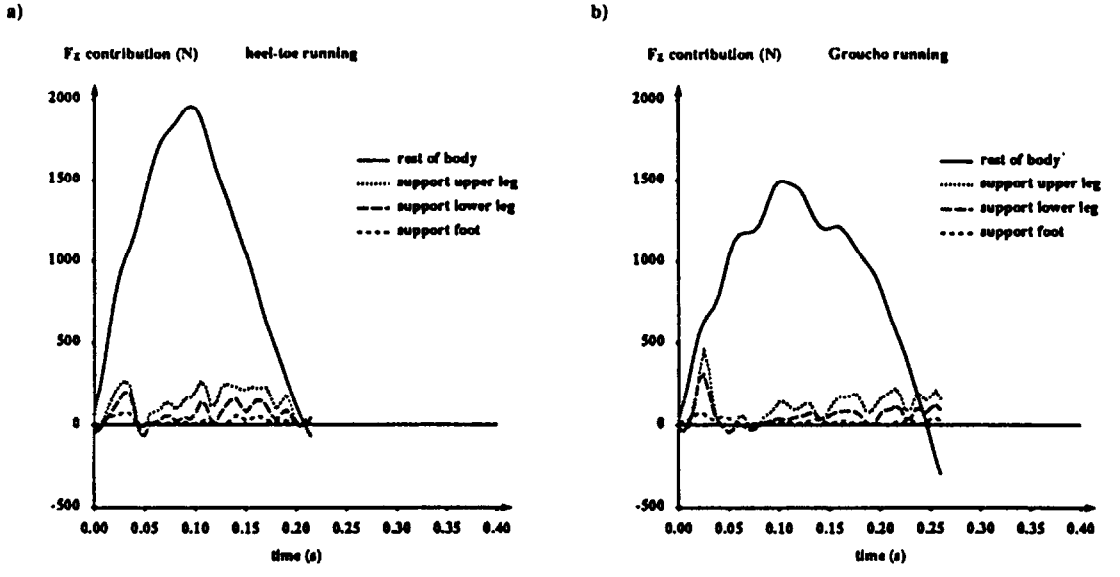

Fig. 10. Segmental contributions to time histories of the vertical ground reaction force F_z, obtained by decomposing the calculated $F_z(t)$. Results in (a) and (b) correspond to results in (a) and (b) of Fig. 8.

the view of the lateral camera before take-off (it became hidden by the upper arm). In these trials, $F_z(t)$ could be calculated only for the very first part of the contact phase.

Segmental contributions to $F_z(t)$

Figure 10(a, b) shows time histories of segmental contributions to $F_z(t)$ for the trials depicted in Fig. 8(a, b), which represents respectively normal running and 'Groucho running' (running while keeping the mass center of the body low, as described by McMahon *et al.*, 1987). For clarity, the contributions of HAT and swing leg are summed to 'rest of the body'.

Figure 10 shows that the first peak in $F_z(t)$ originates from a high-frequency force peak in the contribution of segments of the support leg. This peak is superimposed on a low-frequency, more or less sinusoidal, upward acceleration of the rest of the body. The absolute force value reached by the first peak in $F_z(t)$ depends on both contributions, with the one of the rest of the body being by far the biggest in normal running [Fig. 10(a)]. Note that when the subject changes from normal running to Groucho running, the contribution of the support leg segments to the first peak in $F_z(t)$ increases, whereas that of the rest of the body decreases. In the Groucho running trial, the vertical

velocity of the mass center of the lower leg at touch-down was $-1.4\,m\,s^{-1}$ and that of the mass center of HAT was $-0.9\,m\,s^{-1}$. In the normal running trial the corresponding values were $-1.2\,m\,s^{-1}$ and $-1.2\,m\,s^{-1}$, respectively.

DISCUSSION

Comparison of measured and calculated $F_z(t)$ *curves*

The purpose of this study was to calculate segmental contributions to $F_z(t)$ using accelerations estimated from positional data. In order for this calculation to be successful, three conditions have to be satisfied. The first is that changes in marker positions over time contain information about motion of the center of mass of the segment to which they are attached (i.e. the rigid-body model should apply), the second condition is that marker position time histories are monitored in such a way that the information of interest is retained, and the third condition is that the method of processing the positional data ensures that this information is properly extracted. It was demonstrated that when the high-frequency force peak in $F_z(t)$ immediately after touch-down is to be reconstructed, the second and third conditions could be satisfied using a sampling frequency of 200 Hz and a cutoff frequency of 50 Hz (Fig. 5). In this context it should be noted that the requirement of a high cutoff frequency was overlooked in at least one study. Miller and Nissinen (1987) used cutoff frequencies of 7–9 Hz in an attempt to calculate vertical ground reaction forces for gymnasts pushing off for a forward somersault. They concluded that only the low-frequency components of the ground reaction forces could be derived accurately from positional data. However, no attention was paid to the actual frequency content of the force time histories, and the failure to derive high-frequency components might be due to choosing too low cutoff frequencies. Thus, the question whether marker position time histories can be used for the calculation of segmental contributions to high-frequency peaks in $F_z(t)$ still needs to be answered. Since it was shown in the present study that the method of collecting and processing positional data can be sufficiently accurate, the answer to the question depends on the extent to which changes in marker positions over time reflect motion of the mass center of the segment to which they are attached.

Since the soft tissue mass of a body segment may move relative to the bony structures (Denoth *et al.*, 1985; Gruber *et al.*, 1987), the segmental mass center does not have a fixed anatomical location. Its acceleration will lie somewhere between the acceleration of the bony structures and that of the soft tissue mass. To further complicate matters, both the bony structures and the soft tissue mass are covered by the skin, which may have a different acceleration altogether, especially in impact situations. In horses, the movement of the skin relative to the bone has been shown to be considerable, even in the distal parts of the limbs where the amount of soft tissue is small (van Weeren *et al.*, 1988). In order to minimize possible errors due to this latter factor, special precautions were taken in the present study. The markers used for the lower extremities were mounted rigidly on wooden rods and these rods were fixed to the skin over the whole length of the leg segments. Furthermore, a marker was located at the sternum and fixed to the skin with long strips of tape, and a marker was put on top of the head where vertical acceleration of the skin relative to the underlying tissue is unlikely to occur during running. Still, it seems that the calculation of accelerations of segmental mass centers and associated forces from marker position time histories can only be successful if the accelerations of bony structures and soft tissue mass are not too far apart.

In order to evaluate the accuracy of calculated segmental contributions to $F_z(t)$, time histories of the sum of the segmental contributions were compared to $F_z(t)$ measured directly by a force plate. In the first attempt all marker position time histories were filtered with $f_c = 50$ Hz. Because of the limitations imposed by the relatively low sampling frequency of 200 Hz, the calculated $F_z(t)$ was expected to have a lower first peak than the measured $F_z(t)$ (Fig. 4), but the reverse was found [Fig. 7(a)]. Together with the large fluctuations occurring after the first peak, these findings suggest that, in spite of the precautions taken in this study, sinusoidal accelerations of markers relative to the mass centers of segments still occurred after impact. (The possibility of their being filtering artifacts was ruled out; similar oscillations were already present in the unsmoothed positional data of, for instance, the sternum marker.) Without losing the first force peak, the amplitude of the fluctuations could be reduced by lowering the f_c used in filtering the position time histories of HAT markers [Fig. 7(c)]. This result may be interpreted as follows. The first peak in $F_z(t)$ has its origin in acceleration of the support leg segments (Fig. 10) and is calculated accurately. The fluctuations in the calculated $F_z(t)$ occurring after the first peak have their origin in the contribution of HAT [the remainder of such fluctuations can be seen clearly in Fig. 10(b)]. They seem to be due to sinusoidal marker accelerations relative to the mass center of HAT, and thus constitute errors in calculating the contribution of HAT to $F_z(t)$. The magnitude of these errors can be decreased by lowering f_c. Note that the errors are not due to noise in the position time histories, but represent real accelerations of markers. The problem is that these marker accelerations do not reflect accelerations of the mass center of HAT.

Of course it cannot be proven that the above interpretation is correct and that segmental contributions to $F_z(t)$ are calculated accurately, simply because the actual accelerations of segmental mass centers cannot be measured. Comparing measured and calculated $F_z(t)$ curves seems to be the best we can do to evaluate the accuracy of the method of calculating segmental contributions from positional data. By

varying running style and running speed a wide variety of $F_z(t)$ curves was obtained (examples shown in Fig. 8), and the first peak in the calculated $F_z(t)$ never differed >10% in magnitude and never >5 ms in time of occurrence from the first peak in the measured $F_z(t)$. These results at least give no reason to reject the interpretation that segmental contributions were calculated accurately from positional data. It seems that a mechanical analysis of the landing phase is indeed possible.

Segmental contributions to $F_z(t)$

From the segmental contributions to $F_z(t)$, it became obvious that the frequency characteristics of the first peak in $F_z(t)$ are determined primarily by the accelerations of support leg segments, with the absolute force value reached during the peak depending primarily on the contribution of the rest of the body. An interesting finding is that the contributions of segments of the support leg and the contribution of the rest of the body can be varied independently, as demonstrated in Fig. 10. When the subject changed from normal running [Fig. 10(a)] to Groucho running [Fig. 10(b)], the contribution of the support leg segments to the first peak in $F_z(t)$ increased, whereas that of the rest of the body decreased. A similar observation was made by McMahon *et al.* (1987). The increased force contribution of the leg segments in Groucho running may be attributed to the higher downward velocity of the leg segments at touch-down; a higher velocity means a larger momentum, and consequently a larger impulse is needed to reverse the downward movement of segments of the support leg. The lower force contribution of the rest of the body is explained by a smaller downward velocity of HAT at touch-down in Groucho running. Because the segmental contributions can be varied independently, it is not possible to draw conclusions about segmental contributions from $F_z(t)$. This becomes obvious from the comparison of normal running with Groucho running. In Groucho running the contributions of the support leg segments to the first peak in $F_z(t)$ are greater than in normal running (Fig. 10), but the magnitude of the first peak in $F_z(t)$ is actually lower than in normal running (Fig. 8).

In the literature, it has been hypothesized that the high-frequency peak in $F_z(t)$ during running plays a role in the development of pain and injuries in runners (e.g. James *et al.*, 1978; Clement *et al.*, 1981). In order for this hypothesis to be plausible, it must be assumed that the harmful effects are due to frequency characteristics of the force peaks, or the rate of change of force (i.e. the third position derivative or 'jerk' (Woltring, 1985), and not to the absolute force level reached during the peak. After all, higher force levels are reached later on during the stance phase. A major question to be answered in a mechanical analysis of the landing phase in running is to what extent the high-frequency peak in $F_z(t)$ is 'seen' by the different joints of the body. This question can be answered using the segmental contributions to $F_z(t)$. The resultant intersegmental force occurring in a joint is the sum of the force contributions of segments proximal to the joint. For instance, the resultant intersegmental force occurring in the knee joint of the support leg is the sum of the contributions of the upper leg and the rest of the body to $F_z(t)$. A high-frequency peak is found in the contribution of the upper leg but not in the contribution of the rest of the body. Thus, along the lines of what is said above, the peak in the contribution of the upper leg might play a role in the development of pain and injuries in the knee joint. Since a higher peak in this contribution does not necessarily lead to a higher peak in $F_z(t)$ [Figs 8(a, b) and 10(a, b)], $F_z(t)$ does not provide the relevant information. It follows that if the possible relationship between 'impact force peaks' and injuries is to be investigated, or if the effects of running shoe and surface construction on these force peaks are to be evaluated, the calculation of segmental contributions to $F_z(t)$ is a more suitable approach than measuring only $F_z(t)$. In this context, it is good news that satisfactory results can be obtained with only one camera (Fig. 9).

Acknowledgements—The authors would like to thank Dr M. R. (Fred) Yeadon for his helpful comments on the manuscript and Mr C. W. W. Onderdelinden for his help in collecting the data. This study was supported by grant No. 8345 of the Alberta Heritage Foundation for Medical Research, grant No. N90-123 of the Netherlands Organization for Scientific Research (N.W.O.), and by grant No. OGPIN-001 from the Natural Sciences and Engineering Research Council of Canada.

REFERENCES

Bobbert, M. F. and Schamhardt, H. C. (1989) Explanation of the impact force peak in running. In *Proceedings of the First World Congress on Sport Sciences*, pp. 318–319. U.S.O.C., Colorado Springs.

Cavanagh, P. R. and LaFortune, M. A. (1980) Ground reaction forces in distance running. *J. Biomechanics* **13**, 397–406.

Clauser, C. E., McConville, J. T. and Young, J. W. (1969) *Weight, Volume and Center of Mass of Segments of the Human Body*, pp. 59–60. Wright-Patterson Air Force Base, OH (ARML-TR-69-70).

Clement, D. B., Taunton, J. E., Smart, G. W. and Nicol, K. L. (1981) A survey of overuse running injuries. *Phys. Sportsmed.* **9**(5), 47–58.

Dekel, S. and Weissman, S. L. (1978) Joint changes after overuse and peak overloading of rabbit knees *in vivo*. *Acta orthop. scand.* **49**, 519–528.

Denoth, J., Gruber, K., Keppler, M. and Ruder, H. (1985) Forces and torques during sports activities with high accelerations. In *Biomechanics: Current Interdisciplinary Research* (Edited by Perren, S. M. and Schneider, E.), pp. 663–668. Martinus Nijhoff, Amsterdam.

Dickinson, J. A., Cook, S. D. and Leinhardt, T. M. (1985) The measurement of shock waves following heel strike while running. *J. Biomechanics* **18**, 415–422.

Frederick, E. C., Hagy, J. L. and Mann, R. A. (1981) Prediction of vertical impact force during running. *J. Biomechanics* **14**, 498.

Furnée, E. H. (1989) TV/Computer motion analysis systems: the first two decades. Ph.D. thesis, Delft University of Technology, The Netherlands.
Gruber, K., Denoth, J., Stuessi, E. and Ruder, H. (1987) The wobbling mass model. In *Biomechanics X-B, International Series on Biomechanics*, Vol. 6B (Edited by Jonsson, B.), pp. 1095–1099. Human Kinetics, Champaign, IL.
James, S. J., Bates, B. T. and Osternig, L. R. (1978) Injuries to runners. *Am. J. Sports Med.* **6**, 40–50.
Light, L. H., McLellan, G. E. and Klenerman, L. (1980) Skeletal transients on heel strike in normal walking with different footwear. *J. Biomechanics* **13**, 477–480.
McMahon, T. A., Valiant, G. and Frederick, E. C. (1987) Groucho running. *J. appl. Physiol.* **62**, 2326–2337.
Miller, D. I. and Nissinen, M. A. (1987) Estimation of ground reaction force in the running forward somersault. *Int. J. Sports Biomechanics* **3**, 189–206.
Nigg, B. M., Bahlsen, H. A., Luethi, S. M. and Stokes, S. (1987) The influence of running velocity and midsole hardness on external impact forces in heel–toe running. *J. Biomechanics* **20**, 951–959.
Radin, E. L., Ehrlich, M. G., Chernack, R., Abernathy, P., Paul, I. L. and Rose, R. M. (1978) Effect of repetitive impulsive loading on the knee joint of rabbits. *Clin. Orthop.* **131**, 288–293.
Radin, E. L., Parker, H. G., Pugh, J. W., Steinberg, R. S., Paul, I. L. and Rose, R. M. (1973) Response of joints to impact loading. III. *J. Biomechanics* **6**, 51–57.
Serink, M. T., Nachemson, A. and Hansson, G. (1977) The effect of impact loading on rabbit knee joints. *Acta orthop. scand.* **48**, 250–262.
Voloshin, A. and Wosk, J. (1982) An *in vivo* study of low back pain and shock absorption in the human locomotor system. *J. Biomechanics* **15**, 21–27.
Weeren, P. R. van, Van den Bogert, A. J. and Barneveld, A. (1988) Quantification of skin displacement near the carpal, tarsal and fetlock joints of the walking horse. *Equine Vet. J.* **20**, 203–208.
Woltring, H. J. (1984) On methodology in the study of human movement. In *Human Motor Actions—Bernstein Reassessed* (Edited by Whiting, H. T. A.), pp. 35–73. Elsevier, Amsterdam.
Woltring, H. J. (1985) On optimal smoothing and derivative estimation from noisy displacement data in biomechanics. *Hum. Movmt Sci.* **4**, 229–245.
Wosk, J. and Voloshin, A. (1981) Wave attenuation in skeletons of young healthy persons. *J. Biomechanics* **14**, 261–267.

APPENDIX

Transfer functions of estimators for first and second derivatives

The estimator used in this paper for the first time derivative was:

$$\hat{\dot{x}}(nT) = \frac{(x(nT+T) - x(nT-T))}{2T}, \tag{A1}$$

where n is the sample index, and T is the time between two samples. Suppose we use a discrete input $x(nT)$, given by $[x(nT)] = 0, 1, 0, 0, \ldots$ With initial condition $x(-T) = 0$ the output $\hat{\dot{x}}(nt)$ will be $[\hat{\dot{x}}(nT)] = 1/(2T), 0, -1/(2T), 0, \ldots$ Laplace transformation of $x(nT)$ and $\hat{\dot{x}}(nT)$ yields:

$$X(j\omega) = \mathcal{L}\{[x(nT)]\} = e^{j\omega T}$$

and

$$\hat{\dot{X}}(j\omega) = \mathcal{L}\{[\hat{\dot{x}}(nT)]\}$$

$$= \frac{1}{2T} - \frac{1}{2T} e^{-2j\omega T},$$

with $j \doteq \sqrt{(-1)}$. Thus, the transfer function equals:

$$H(j\omega) = \frac{\hat{\dot{X}}(j\omega)}{X(j\omega)} = \frac{1}{2T}(e^{j\omega T} - e^{-j\omega T}) = \frac{1}{T} j \sin \omega T,$$

whereas the ideal transfer function of an estimator for the first time derivative is $j\omega$. The ratio $H_1(\omega T)$ of these two transfer functions is:

$$H_1(\omega T) = \frac{\sin(\omega T)}{\omega T} = \frac{\sin(2\pi f T)}{2\pi f T}, \tag{A2}$$

where f is signal frequency.

For the estimator used in this paper for the second time derivative, i.e.

$$\hat{\ddot{x}}(nT) = \frac{(\hat{\dot{x}}(nT+T) - \hat{\dot{x}}(nT-T))}{2T} \tag{A3}$$

the ratio $H_2(\omega T)$ equals:

$$H_2(\omega T) = (H_1(\omega T))^2 = \left(\frac{\sin(2\pi f T)}{2\pi f T}\right)^2. \tag{A4}$$